International Journal of Science and Research (IJSR)
ISSN (Online): 2319-7064
Impact Factor (2012): 3.358

Fabrication and Analysis of Nanocrystalline Superconductor YSrBiCuO at Different Calcination Temperatures

Anusha Mony[1], Jayakumari Isac[2]

[1, 2]Centre for Condensed Matter, Department of Physics, CMS College, Kottayam, India

Abstract: ***Tremendous interest has developed over the past two decades in understanding as well as utilizing in a variety of applications with the discovery of high-TC superconducting materials like Yttrium Barium Cupric Oxide, Bismuth Strontium Calcium Copper Oxide and Thallium Calcium Barium Copper Oxide. The thin films of these materials are expected to play an important role in the area of microelectronics, especially for interconnects in integrated circuits, Josephson junctions, magnetic field sensors and optical detectors. In this work, the authors designed a new nanocrystalline ceramic type II high-TC superconductor, Yttrium strontium bismuth Copper Oxide (YSrBiCuO/YSBCO). The YSBCO was prepared by the solid state thermo chemical reaction technique involving mixing, milling, calcination and sintering. In order to show the viability of the proposed method, super-conducting powder was prepared in special furnace. The sample was analyzed by X-Ray Diffraction (XRD), an indispensible non-destructive tool for structural materials characterization and quality control which makes use of the Debye-Scherrer method. The comparison of XRD results with JCPDS files and applying XPERT-PRO software confirmed the orthorhombic structure of the sample. X-ray instrumental peak broadening analysis was used to evaluate the size and lattice strain by the Williamson-Hall Plot method. It was characterized by using Scanning Electron Microscopy (SEM) which revealed that its particle size is in the nanometer and confirmed the calculated value of particle size from Debye Scherrer's formula. EDX plot shows the presence of all the constituents. Dislocation density (δ) also is calculated.***

Keywords: YSrBiCuO, nanocrystalline, Debye Scherrer, Williamson-Hall, Dislocation density, EDAX

1.Introduction

High-temperature superconductors (abbreviated **high-T_c** or **HTS**) have been observed with transition temperatures as high as 138 K (−135 °C).[1] Until 2008, only certain compounds of copper and oxygen (so-called "cuprates") were believed to have HTS properties, and the term high-temperature superconductor was used interchangeably with cuprate superconductor for compounds such as bismuth strontium calcium copper oxide (BSCCO) and yttrium barium copper oxide (YBCO). However, several iron-based compounds (the iron pnictides) are now known to be superconducting at high temperatures.[2][3][4] After more than twenty years of intensive research the origin of high-temperature superconductivity is still not clear, but it seems that instead of electron-phonon attraction mechanisms, as in conventional superconductivity, one is dealing with genuine electronic mechanisms (e.g. by antiferromagnetic correlations), and instead of s-wave pairing, d-waves are substantial. One goal of all this research is room-temperature superconductivity[5] .Since there is a complete expulsion of magnetic flux, superconductors are perfectly diamagnetic [6] [7]. High-voltage generator can be developed by using HTS inductor and electronic RCL series resonant circuit [8] [9].

A lot of reports are there of BSCCO [10-13] and YBCO as a new class of superconductor. There have been only minor improvements to these materials since. A key early development was to replace about 15% of the Bi by Pb, which greatly accelerated the formation and quality of Bi-2223. The different families differ in the structure between the planes and also in the number of Copper-Oxide planes in the unit cell. There are materials with two consecutive Copper-Oxygen planes (these are denominated "bilayer superconductors"), and some with more consecutive planes (multilayer materials) in the unit cell. Because of the presence of the Copper-Oxygen planes, and their importance, as all the cool action happens in the planes, these materials are colloquially known as "cuprates".

Ions may be larger or smaller than the neutral atom, depending on the ion's charge. When an atom loses an electron to form a cation, the lost electron no longer contributes to shielding the other electrons from the charge of the nucleus; consequently, the other electrons are more strongly attracted to the nucleus, and the radius of the atom gets smaller. Similarly, when an electron is added to an atom, forming an anion, the added electron shields the other electrons from the nucleus, with the result that the size of the atom increases[14].

In this work the authors describe the fabrication of YSrBiCuO nano crystalline ceramic type II high-TC superconductor material by the solid state thermo chemical reaction technique similar to substituting Ca (114pm) of BSCCO by Yttrium (104pm) and it is characterized to show good quality, homogeneity and the desired stoichiometry of the sample prepared. The results were analyzed by X-Ray Diffraction (XRD), SEM, and EDX. The particle size was determined from XRD details by Debye Scherrer formula. The SEM studies revealed that its particle size is in hundred-nanometer range. The EDX spectrum of YSBCO gave the information on the elemental composition of the material. Using Instrumental Broadening and Williamson-Hall Plot method the particle size and strain of the material were found. Line profile analysis (LPA) refers to the analysis of the shape of the peaks. Dislocation density (δ) an important material property, which gives the length of the dislocations present per unit volume (m/m3) of the sample. This strongly affects the out-of-pile and in-pile properties of materials[15] .

2.Materials and Experimental Methods

The nano-sized ceramic material YSBCO has perovskite structure. The perovskite compounds are cubic and the variants are tetragonal and orthorhombic and have the chemical formula ABO_3. The most familiar ceramic superconducting materials have perovskite structure[16]. According to the chemical formula, the YSrBiCuO (YSBCO) (figure 1) was prepared by the thermo chemical solid state reaction technique using a high-energy ball milling process through mechanically assisted synthesis. For preparing the sample, the reagent grade chemicals of high purity Yttrium Oxide, strontium Carbonate, bismuth oxide, cupric oxide powders were used as the raw materials and weighed according to their molecular formula. The powders of the required ceramics were mixed mechanically. Mechanical mixing is usually done by hand mixing in agate mortar for very long time. The sample was ball milled for three weeks with suitable zirconium balls to insure homogeneity and quality. Then it was attrition milled for five hours. Then the material calcined at different temperatures, 30˚C, 500˚C, 800˚C and 950˚C. After the furnace is off, on cooling the oxygen is allowed to flow into the furnace at intervals (oxygen annealing). A final furnace temperature of 950˚C is maintained for the intermediate firings. A temperature much higher than this will result in a material that is much harder to regrind.

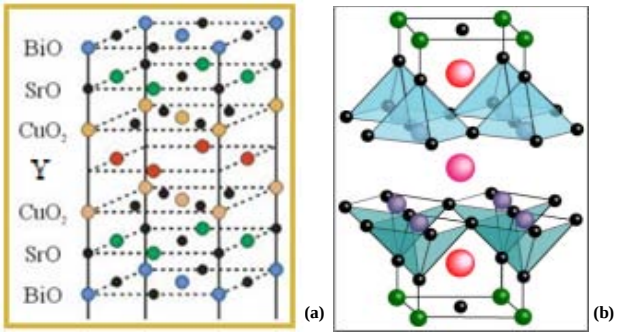

Figure 1: Crystal Structure of YSrBiCuO (a) & (b) (b) Copper-Oxide layer, shown in purple and Oxygen in brown. Bismuth in green, Yttrium in pink and Strontium in orange

Each sample was analyzed by the X-Ray diffraction spectrum. X-ray diffraction spectrum of these materials was taken using Bruker AXS D8 advance diffractometer. The diffractometer with radiations of wavelength 1.541A˚ having Nickel filter, equipped with X-ray generator 1140/90/96 having X-ray source KRISTALLOFLXE 780, KF, 4KE with wide angle goniometer PW1710/70 with single pen recorder pm 8203 and channel control PW1390 at 35kV, 10 mA is used for the purpose. The scanning speed of the specimen is 2 degree/minute. From the XRD results, it was concluded that this crystal was found to be orthorhombic system. The different methods used to evaluate the crystallite size of the sample are given below. The crystallite sizes of samples were calculated from the XRD data by the Debye Scherrer method, Williamson Hall analysis and size-strain plot method.

2.1 Scherrer Method

The particle size and crystal morphology play important roles in application level of ceramic materials. So their studies are very important in the ceramic research field. No crystals are perfect due to their finite size, because a perfect crystal would extend infinitely in all directions. This leads to the broadening of the diffraction peaks. The two main properties extracted from peak width analysis are (a) crystallite size and (b) lattice strain. Crystallite size is a measure of the size of a coherently diffracting domain. Lattice strain is a measure of the distribution of lattice constants arising from crystal imperfections, such as lattice dislocation[17,18] . The lines in a powder diffraction pattern are of finite breadth but since the particles were very small, the lines started to broaden than usual. The broadening decreases with the increase in crystallite size. The crystallite size for YSrBiCuO is calculated from X-ray diffraction profiles of strong reflections with intensity % by measuring the full width at half maximum (FWHM). X-ray diffraction profile is used to measure the average crystallite size of the sample provided the average diameter was less than 200 Å. The Debye Scherrer equation for calculating the crystallite size is given by $\boldsymbol{D = \frac{K\lambda}{\beta cos\theta}}$ **(1)** [19] where K is the Scherrer constant, λ is the wavelength of light used for the diffraction, β the "full width at half maximum" of the sharp peaks, and θ the angle measured. The Scherrer constant (K) in the above formula accounts for the shape of the particle and is generally taken to have the value 0.9. From the results it ia concluded that the crystallite size is less than 100 nm. The XRD diffraction profile of YSBCO at temperatures 30˚C, 800˚C & 950˚C are given below in Fig.2. Table 1 gives the hkl indices corresponding to 2θ values. The particle sizes of YSBCO calculated at various d /2θ values of different temperatures are shown in the Table2. Increase in particle size with treating temperatures, diffraction angle theta shifting to right on increase of calcinations temperature of the sample and band width β decreasing on increasing calcinations temperature of the sample YSrBiCuO can be visualized in the Fig.3.

Comparing the XRD data with JCPDS file and applying XPERT- PRO software it is concluded that YSBCO have an orthorhombic system, details furnished below.

a ≠ b ≠ c and α = β = γ = 90˚. -- Orthorhombic system.
a =12.4198**A**◦**, b = 6.8953**A◦ **, c = 6.5708A◦. Cell volume =562.7101**^{03}

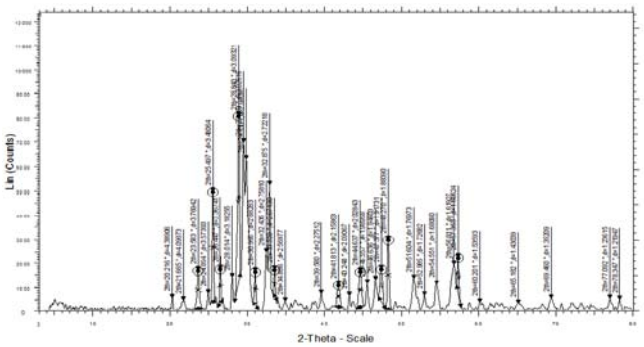

(a)

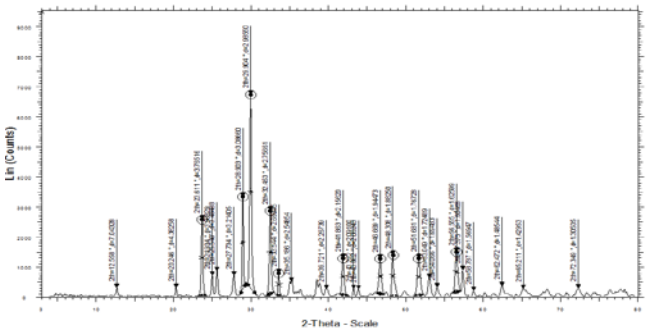

(b)

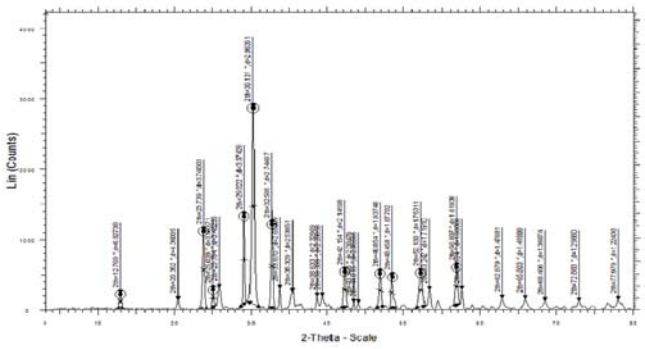

(c)

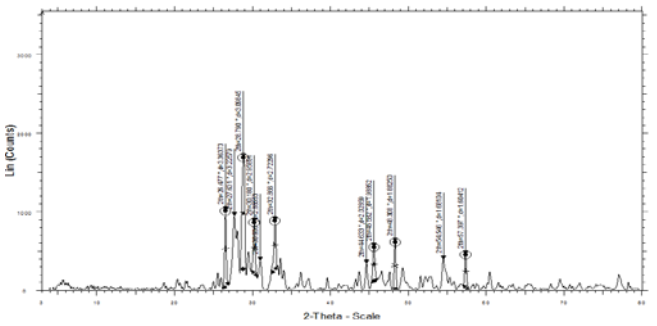

(d)

Figure 2: shows the XRD diffraction profile of YSBCO at temperatures (a) 30◦C, (b) 5000C, (c) 800◦C & (d) 950◦C.

Table 1: The (hkl) indices calculated from the 2 θ values of the XRD profile are listed below .

2 θ in degrees	hkl
27.734	(002)
28.930	(311)
29.904	(021)
30.996	(202)
32.453	(410)
33.520	(212)
33.544	(320)
45.557	(330)
46.669	(601)
48.308	(313)
51.681	(123)
53.049	(602)
54.066	(041)
56.555	(503)
57.375	(340)

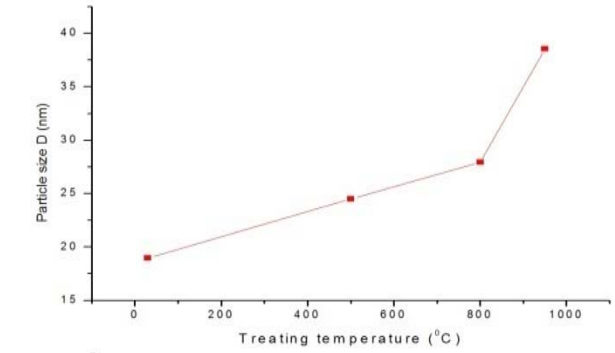

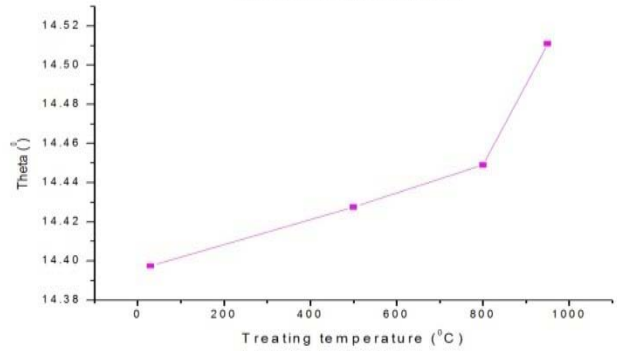

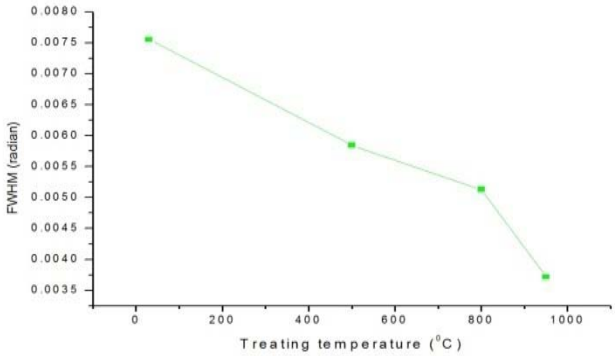

Figure 3: shows particle size increase/variation, angle of diffraction shifting to right, β the band width decrease with respect to increase in calcination temperature of the sample YSrBiCuO.

Peak broadening with crystallite size can be studied from the XRD data analysis. Crystals formed may not be perfect due to their finite size. The disparity or deviations from perfect crystallinity leads to the broadening of the diffraction peaks. The two main factors of peak width analysis are the crystallite size and lattice strain. Hence the 2θ peak positions get shifted. The breadth of the Bragg peak is a combination of both instrument and sample dependent effects as

$$\beta^2_{\text{crystallite size}} = \beta^2_{\text{measured}} - \beta^2_{\text{instrumental.}} \text{ ----------(2)}$$

Therefore D = K λ / β cos θ => cos θ K λ/D(1/ β)

2.2 Scherrer Plot Method

The treating temperature changes also affect on the particle size and strain of YSBCO. This change reflects on the XRD spectrum. Due to the temperature change the peak width and intensity of the peak changed and also 2Θ peak position shifted. The crystallite size varies as 1/cos θ and stain varies as tan θ from the peak width. This difference in behavior as a function of 2q enables one to discriminate between the size and strain effects on peak broadening. The Bragg width

contribution from crystallite size is inversely proportional to the crystallite size[20].

Scherrer Plots were drawn with 1/ β on the X-axis and cos θ along the Y-axis at different temperatures as given in the Fig.3.

By linear fitting the data, the crystallite size D was extracted from the slope of the line.

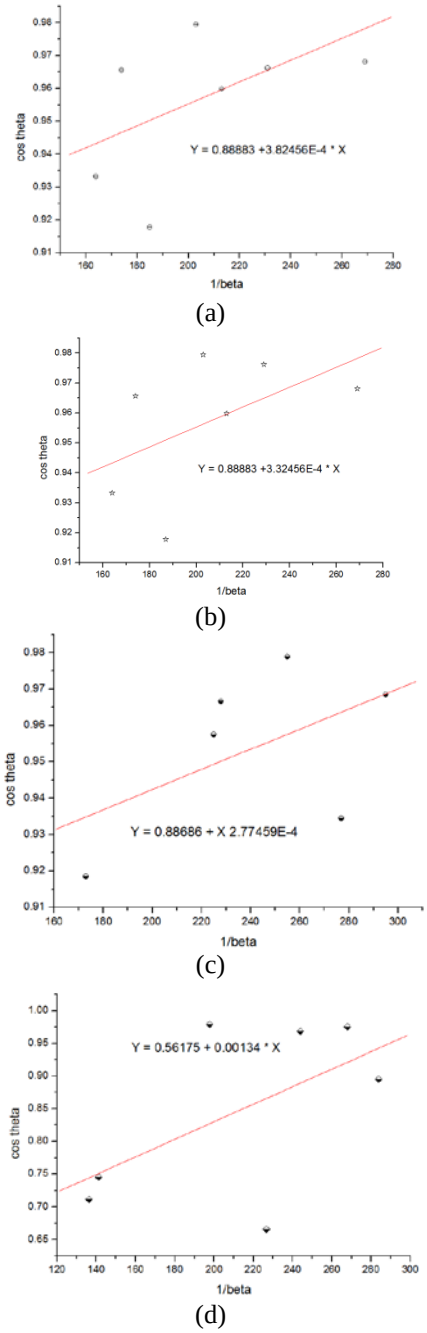

Figure 4: shows the Scherrer plots of YSBCO at different temperatures (a,b,c,d: at 30^0C,500^0C,800^0C,950^0C)

2.3 Wiliamson- Hall (W-H) Plot Method

W-H plot and size-strain plot method used to study the changes of the strain and size with respect to the temperature.W-H analysis is a simplified integral breadth method where size-induced and strain-induced broadening are deconvoluted by considering the peak width as a function of 2 θ[21].W-H plots emphasised the strain induced plots. The peak width derived from crystallite size varies as 1/cos θ whereas strain varies as tan θ. This difference in behaviour as a function of 2 θ enables to distinguish between the size and strain effects on peak broadening. The Bragg width contribution from crystallite size is inversely proportional to the crystallite size [22].

Addition of Scherrer formula and the strain induced broadening results in

$\beta^2_{hkl} = K\lambda/D\cos\theta + 4\varepsilon \tan\theta$ ------(3) **where ε** represents the strain.

W-H plots are drawn with β cos θ along the Yaxis and 4sin θ along the X axis as given in Figure 5. The slope and Y-intersect of the fitted line represent strain and particle size, respectively.

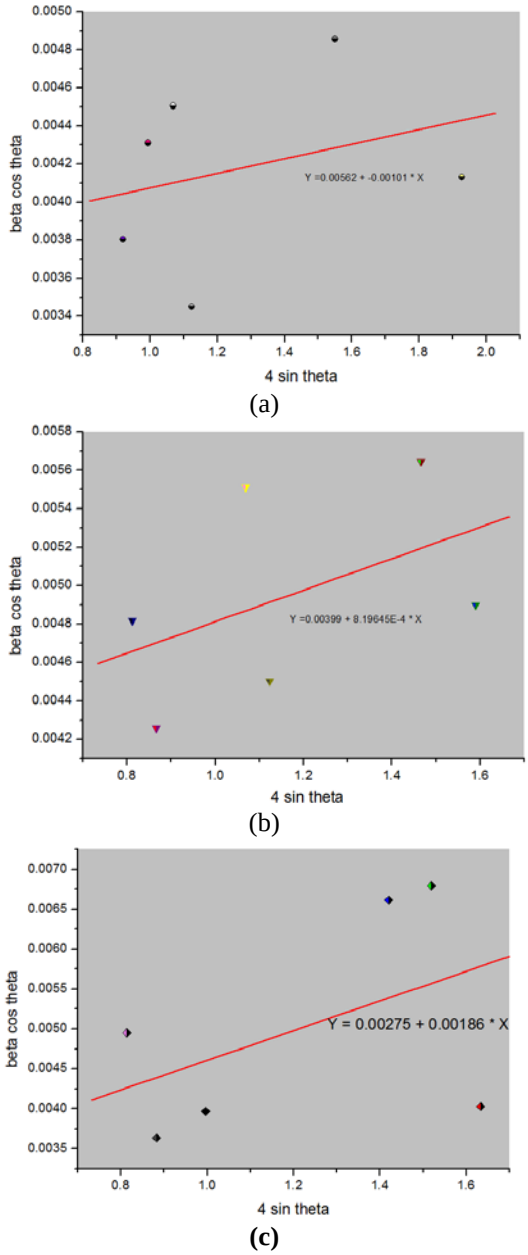

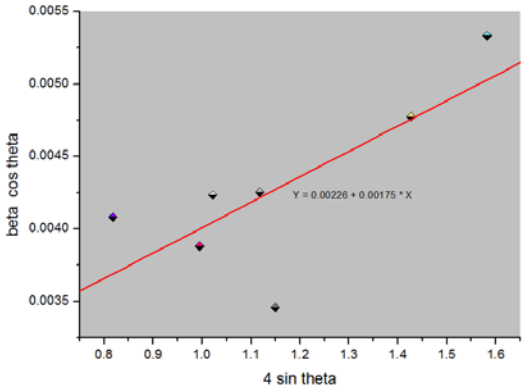

(d)

Figure 5: represents the W-H plots of YSBCO at different temperatures: (a,b,c,d: at 30^0C,500^0C,800^0C,950^0C)

2.4 Size-Strain Plot Method

The value of d (the inter planar spacing between the atoms) is calculated using the **Bragg's Law**, $2d\sin\theta = n\lambda$ or $d = \frac{\lambda}{2\sin\theta n(n=1)} - - - - (2)$,Wavelength of X ray = 1.5 Å for CuKα.

Williamson-Hall plot has explained that line broadening was basically isotropic. Due to micro strain contribution the diffracting domains are also isotropic. Size-strain parameters can be obtained from the "Size-Strain Plot" (SSP). Here it is assumed that the 'strain profile' is given by Gaussian function and the 'crystallite size' by Lorentzian function [15]. In the plots given below in Fig.4, $d^2_{hkl}\,\beta_{hkl}\cos\theta$ and $(d_{hkl}\,\beta_{hkl}\cos\theta)^2$ were taken on X- axis and Y-axis respectively for all peaks. The crystallite size is calculated from the slope of the linearly fitted data and the root of the Y-intercept gives the strain[23]. The crystallite size D can be measured from the Debye Scherrer formula as **$D=0.9\lambda/\beta\cos\theta$.**

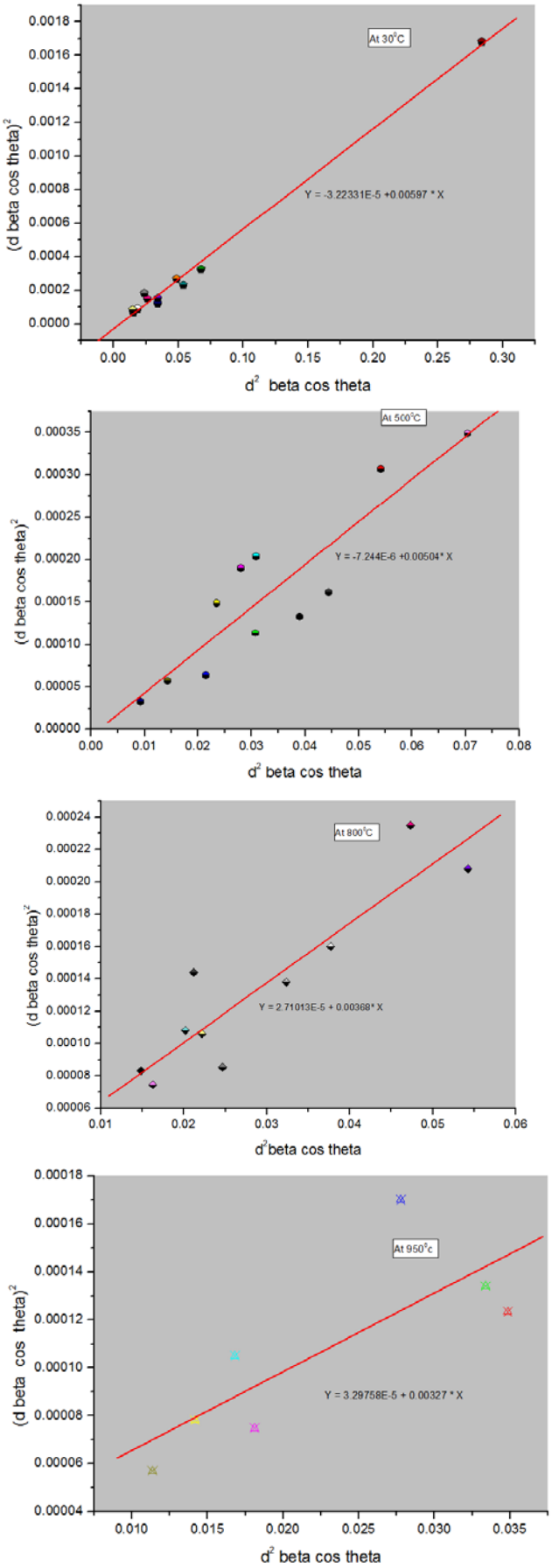

Figure 6: ($\mathbf{d^2_{hkl}\,\beta_{hkl}\cos\theta}$) versus $\mathbf{(d_{hkl}\,\beta_{hkl}\cos\theta)^2}$ plots of YSBCO at different temperatures: at 30^0C,500^0C,800^0C,950^0C .

Table 2: The crystallite size of the sample YSrBiCuO calculated from the different methods are listed below.

Sample YSBCO calcined at different temperatures	XRD values:2θ in degrees			
	At 30^{0}C	At 500^{0}C	At 800^{0}C	At 950^{0}C
Shifting of peak values of XRD with temperature	25.497 28.840 32.436 41.813 46.636 48.270 51.604 56.311	25.540 29.904 32.453 41.863 46.669 48.308 51.681 56.555	25.784 30.131 32.595 42.154 46.854 48.458 52.130 56.807	26.477 30.180 -- 32.866 -- -- 48.308 57.397
Average Particle size in nm: By theoretical Calculation From Scherrer plot From W-H graph From Size-Strain Plot	*18.9593* *21.862* *24.1* *22.6*	24.51255 25.9071 33.83 26.78	27.93188 30.5563 49.09 37.56	38.56740 46.4532 59.73 41.041
Strain from: W-H graph Size-Strain Plot	*0.00101* *0.01794*	0.000819 0.00848	0.00186 0.0164	0.00175 0.0181

The crystallite size of the sample YSrBiCuO calculated from the different methods are plotted in figure 7 for comparison. It is observed that the crystallite size increased with increased calcinations temperature of the sample.

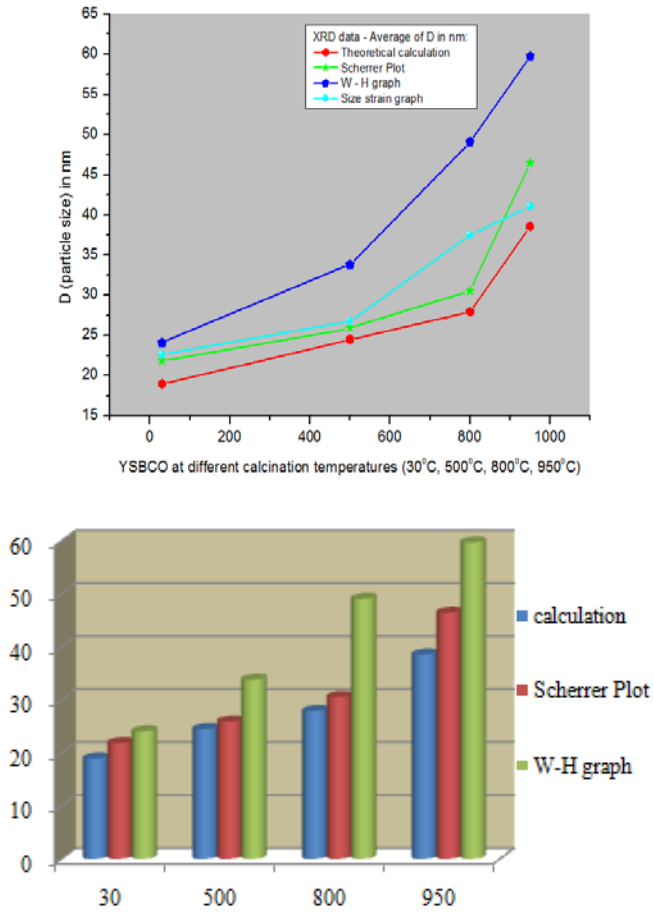

Figure 7: The crystallite size of the sample YSrBiCuO calculated from the different methods.

2.5 XRD-Instrumental Broadening

The observed line broadening will be used to estimate the average size of the particles. When particle size is less than 100 nm, appreciable broadening in X-ray diffraction lines will occur. Diffraction pattern will show broadening because of particle size and strain. The total broadening of the diffraction peak is due to sample and the instrument. The sample broadening is described by

$$FW(s) \times \cos\theta = \frac{K \times \lambda}{size} + 4 \times strain \times \sin\theta$$

The total broadening βt equation is described by

$$\beta_t^2 \approx \left\{\frac{0.9\lambda}{D\cos\theta}\right\}^2 + \{4\varepsilon\tan\theta\}^2 + \beta_0^2$$

Where D is average particle size, ε is strain and βo is instrumental broadening. Instrumental broadening is presented in **Figure.3**.

2.6 XRD- Dislocation Density

The properties of the crystal formed are strongly influenced by the defects inside the crystal. Shift or movement of a dislocation is impeded by other dislocations present in the sample. The dislocation density is defined as the length of dislocation lines per unit volume of the crystal. Chen and Hendrickson measured and determined dislocation density and hardness of several crystals. Theoretically a dislocation is a crystallographic irregularity or a defect formed within the crystal. It is found that crystals with larger dislocation density were harder. It has been shown that the dislocation density increases while crystallite size decreases with increasing strain and ultimately these parameters reach saturation values. Above a certain crystallite size limit (~20 nm) the strength of materials increases with decreasing crystallite size. The dislocation density (δ) in the sample has been determined using values of FWHM, θ, lattice constant and crystallite size. The number of unit cell is calculated from crystallite size and cell volume of the sample [24].

(δ)= 15βcosθ/4aD, where **β,** the FWHM measured in radians**, θ** the diffracting angle, **a** the cell parameter and **D** is the crystallite size in nm. The no. of unit cells**, n=π x(4/3)(D/2)^3 x1/V**, where **V** is the cell volume of the sample(V=**562.7101**^{03}). Fig.8 shows the variation of dislocation density **(δ)** with the crystallite size and no. of unit cells are given below.

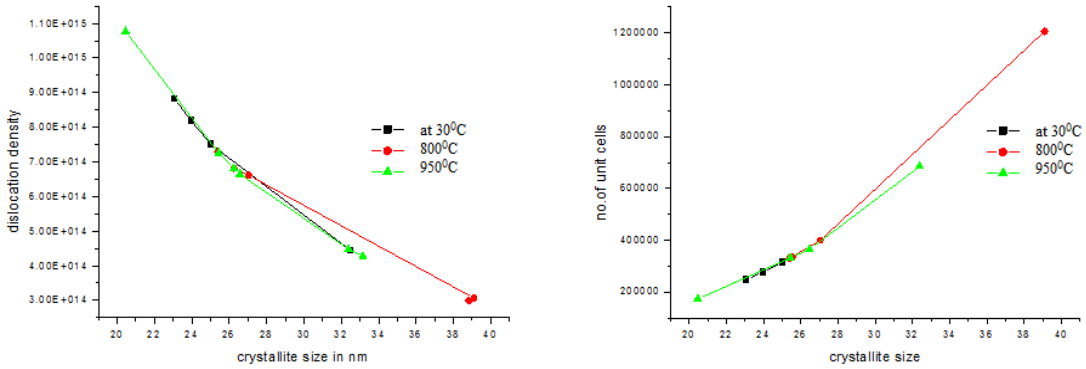

Figure 8: dislocation density vs. crystallite size & no. of unit cells vs. crystallite size of YSBCO

2.7 SEM Analysis

SEM photograph of the sample gives idea about the particle size and it helps to arrive on a the range of particle size. The SEM analyses the surface of solid objects, producing images of higher resolution than optical microscopy and produces topographical image of YSBCO. Fig.9 shows the surface morphology of the sample. The crystallite size measurement through SEM revealed that its maximum dimension is always less than 100nm.

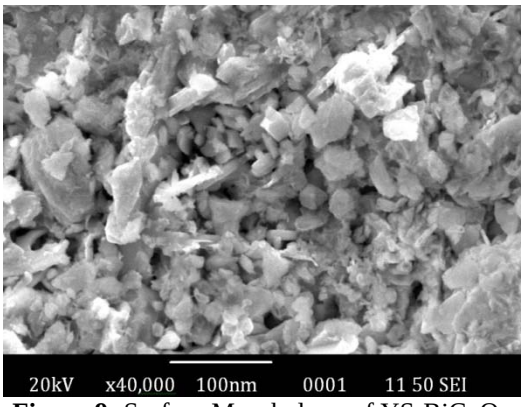

Figure 9: Surface Morphology of YSrBiCuO.

2.8 Energy Dispersed X-Ray Spectrograph (EDX)

EDAX of the sample was recorded using ISIS Link Oxford Instrument UK. EDAX shows the composition details of the prepared ceramic material (Fig.10). This technique is generally associated with Scanning Electron Microscope (SEM). The size of the pulse generated depends on the number electron hole pairs created, which in turn depends on the energy of the incoming X-ray. The detector which is lithium doped silicon is protected by a beryllium window and operated at liquid nitrogen temperatures.

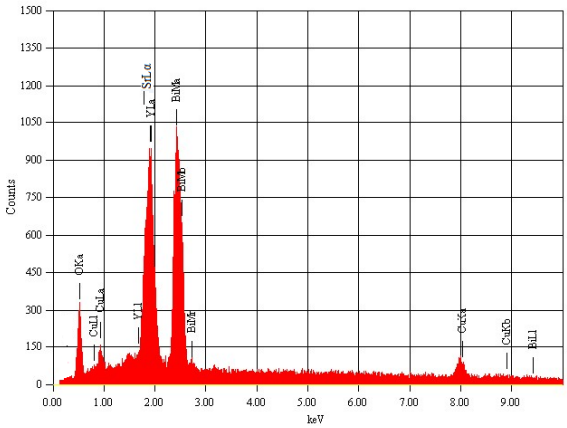

Figure 10: EDAX spectrum of YSrBiCuO

From the EDAX spectrum, the dominant peak positions at 1.922keV (Y Lα), 1.806keV (Sr Lα), 2.419keV (Bi M), 0.930, 8.040keV (Cu Lα, Kα), 0.525keV (O Kα) correspond quite well to the energy pattern of the corresponding materials (Y, Sr, Bi, Cu and O) reported in the EDAX international chart. Percentage composition according to EDAX analysis is shown in table 3.

Table 3: Percentage composition of prepared sample YSrBiCuO

Element	(keV)	Mass%
O K	0.525	3.57
Cu K	8.04	3.81
Y L	1.922	15.35
Sr L	1.806	15.75
Bi M	2.419	61.52
Total		100

3.Results and Discussion

A systematic and detailed analysis of the new perovskite YSBCO was successfully done in this work. XRD spectrum gave a clear idea about the maximum intensity peak shifting corresponds to the different treating temperatures. The XRD patterns of YSBCO sample obtained for various annealing temperatures are shown in Figure 2. As the temperature increases, the highest peaks in the XRD spectrums shift from left to right through the 2θ axis (figure 3). Line Profile Analysis of the sample was carefully carried out to analyze the shape of the diffraction peaks.

The atoms undergo thermal vibration about their mean positions even at the absolute zero of temperature, and the amplitude of this vibration increases as the temperature increases. Increased thermal vibration of the atoms, as the result of an increase in temperature, the unit cell expands, causing changes in d spacing and therefore in the 2θ positions of the diffraction lines. And also the intensities of the diffraction lines decrease. When the material is cooled to room temperature, the amplitude of the atomic vibrations of the material was decreased. But it couldn't arrive at the initial amplitude. The atomic vibration amplitude of the heated material was higher than initial amplitude [25].

Crystals with precise periodicities over long distances have sharp and clear diffraction peaks. Crystals with defects (such as impurities, dislocations, planar faults, internal strains, or small precipitates) are less precisely periodic in their atomic arrangements, but they still have distinct diffraction peaks. Their diffraction peaks are broadened, distorted, and weakened, however, and "diffraction line shape analysis" is an important method for studying crystal defects.

Generally, only lattice distortions affect the peak positions whereas structure defects cause a (perhaps also anisotropic) broadening of peaks only.

1) Shift caused due to the stress, strain, dislocation and defects induced since the synthesis parameters.
2) Irradiation effect (Synthesis parameters) might alter the lattice parameters, which may affect the internal properties of the crystal.

Depend upon the internal properties value, peak position shifted towards higher or lower angle. The shift of diffraction peaks towards higher diffraction angle means crystal lattice is compressed. If the only effect observed is a shift of ALL the Bragg peaks to higher values of the diffraction angle, this means that the lattice parameter is decreasing. Several reason are possible: the increase in annealing temperature may bring about two changes; 1) increase in the crystallite size, and 2) possible formation of new phases. In the first case, increase in crystallite size modifies the preferences of crystallographic lattice sites, and as a result increase in 2 theta means decrease in lattice constant. In the second case, if there are additional phases, the observed peaks would also change. That means, some existing peaks disappear and some new peaks may appear.

From Fig.2, the peak broadening in the XRD patterns clearly indicated the nature of formation of the very small nano ceramic material. Shift in peak towards right is an indication of orthorhombic crystal formation tending the sample to attain superconducting state. From the width of the XRD peak, the mean crystallite size is calculated using Debye Scherrer's equation. The values calculated using the Scherrer formula are compared to the values obtained through Scherrer plot, Williamson-Hall plot and the Size-Strain Plot drawn for various temperatures. The disparity or deviations from perfect crystallinity leads to the broadening of the diffraction peaks and hence the 2θ peak positions get shifted. Results agree with the values obtained from different methods.

From Table 2, it is confirmed that crystallite size of the material YSBCO increases with the treating temperature increase. The diffraction data revealed that the material belongs to orthorhombic system. Heat treatment causes the particles to anneal and form larger grains, which of course indicates that the particles become larger. Hence, the large size of sample at 950˚C is expected. Miller indices, the hkl values calculated from the XRD profile using XPERT –PRO software are listed in the Table.1.

Higher value of dislocation density results in greater hardness. The dislocation density (δ) is determined from the XRD profile. It is clearly confirmed that dislocation density decreases as the crystalline size increases. The no. of unit cells also is found to have an inverse relation with the dislocation density. SEM is an experimental proof of the theoretical calculation of crystallite size by Debye Scherrer equation. Figure.9 shows SEM image of **YSBCO**. The SEM photograph revealed that maximum dimensions of the particles are less than 100 nm. Thus the morphology of particles can be visualized by SEM.

The EDAX analysis indicates that the elements exist in the sample and they agree with the chemical formula of the prepared compound. The EDAX spectrum (figure 10) obtained give the confirmation of the elemental composition of the material (Table 3) under investigation.

4.Conclusion

Nanocrystalline superconducting ceramic YSrBiCuO **was** prepared using the thermo chemical solid state technique and is characterized by XRD and SEM analysis. The XRD line profile analysis indicated the formation of a peroskvite phase at high temperature. The shifting in XRD peak towards right on high annealing temperatures confirms its orthorhombic formation which is a clear indication of its superconducting phase formation. The crystallite size increased as the temperature is increased. The results of broadening analysis by Scherrer plot method, W-H plot method and Size-Strain plot method are in high inter correlation. **.** Characterization with Scanning Electron Microscopy (SEM) revealed that its particle size is in the nanometer and confirmed the calculated value of particle size from Debye Scherrer's formula, W-H and SSP methods. EDX plot confirmed the presence of all the constituents. Dislocation density (δ) also is calculated. A sound understanding of the properties of sample shows that YSBCO will definitely have a future in power electronics and microelectronics.

5.Acknowledgement

The authors are thankful to UGC for the financial Assistance, SAIF, Kochi for providing the instrumental data and to the Principal, CMS College, Kottayam, Kerala for providing the facilities.

References

[1] Ford, P. J. (2005). *The Rise of the Superconductors*. CRC Press.

[2] A. Leggett (2006). "What DO we know about high T_c?". *Nature Physics* **2** (3): 134.Bibcode:2006NatPh...2..134L. doi:10.1038/nphys254.
[3] Choi, Charles Q. Iron Exposed as High-Temperature Superconductor: Scientific American. April 23, 2008.
[4] Ren, Zhi-An; Che, Guang-Can; Dong, Xiao-Li; Yang, Jie; Lu, Wei; Yi, Wei; Shen, Xiao-Li; Li, Zheng-Cai; Sun, Li-Ling; Zhou, Fang; Zhao, Zhong-Xian (2008). "Superconductivity and phase diagram in iron-based arsenic-oxides ReFeAsO1−δ (Re = rare-earth metal) without fluorine doping". *EPL* **83**: 17002. arXiv:0804.2582. Bibcode:2008EL.....8317002R. doi:10.1209/0295-5075/83/17002.
[5] Mourachkine, A. (2004). *Room-Temperature Superconductivity*. Cambridge International Science Publishing.arXiv:cond-mat/0606187. ISBN 1-904602-27-4
[6] Kittel, C. (2004) Introduction to Solid State Physics. 7th Edition, Wiley, India.
[7] Puri, R.K. and Babbar, V.K. (2009) Solid State Physics. S Chand & Company Ltd., New Delhi.
[8] Narlikar, A.V. (2004) High Temperature Superconductivity. Springer, Berlin, 35.
[9] in, J.X. and Dou, S.X. (1999) Development of High TC Superconductors for Engineering Applications. *Science &*
[10] *Technology Advancing into New Millenium*, 368-382.
[11] H. Maeda, Y. Tanaka, M. Fukutumi, and T. Asano (1988). "A New High-T_c Oxide Superconductor without a Rare Earth Element".*Jpn. J. Appl. Phys.* **27** (2): L209–L210. Bibcode:1988JaJAP..27L.209M. doi:10.1143/JJAP.27.L209.
[12] M. A. Subramanian *et al* (1988). "A new high-temperature superconductor: $Bi_2Sr_{3-x}Ca_xCu_2O_{8+y}$". *Science* **239** (4843): 1015–1017.Bibcode:1988Sci...239.1015S. doi:10.1126/science.239.4843.1015. PMID 17815702.
[13] R. J. Cava *et al* (1988). "Structure and physical properties of single crystals of the 84-K superconductor $Bi_{2.2}Sr_2Ca_{0.8}Cu_2O_{8+\delta}$".*Physical Review B* **38** (1): 893–896. Bibcode:1988PhRvB..38..893S. doi:10.1103/PhysRevB.38.893.
[14] J. L. Tallon *et al* (1988). "High-T_c superconducting phases in the series $Bi_{2.1}(Ca,Sr)_{n+1}Cu_nO_{2n+4+\delta}$". *Nature* **333** (6169): 153–156.Bibcode:1988Natur.333..153T. doi:10.1038/333153a0.
[15] R. D. Shannon (1976). "Revised effective ionic radii and systematic studies of interatomic distances in halides and chalcogenides". Acta Cryst A32: 751–767.Bibcode:1976AcCrA..32..751S.doi:10.1107/S0567739476001551.
[16] Willander1, O. Nur1, M. Q. Israr1, A. B. Abou Hamad2, F. G. El Desouky 2, M. A. Salem2, I. K. Battisha2* Determination of A.C. Conductivity of Nano-Composite Perovskite Ba(1–x–y)Sr(x)TiFe(y)O3 Prepared by the Sol-Gel TechniqueM-*Journal of Crystallization Process and Technology*, 2012, 2, 1-11 http://dx.doi.org/10.4236/jcpt.2012.21001 Published Online January 2012 (http://www.SciRP.org/journal/jcpt)
[17] Galasso, F.S. (1969) Structure, Properties and Preparation of Perovskite Type Compounds. Pergamon Press, Oxford.
[18] K. Ramakanth, Basic of Diffraction and Its Application. I.K. International
[19] Publishing House Pvt. Ltd, New Dehli, 2007.
[20] J. Zhang, Y. Zhang, K.W. Xu, V. Ji, Solid State Commun. 139 (2006) 87.
[21]. West, A.R. (1974) Solid State Chemistry and Its Applications. Wiley, New York,
[22] V.K. Pecharsky, P.Y. Zavalij, Fundamentals of Powder Diffraction and Structural
[23] Characterization of Materials. Springer, New York, 2003.
[24] 21. 17 A. Khorsand Zak a,b,*, W.H. Abd. Majid a, M.E. Abrishami b, Ramin Yousefi c- X-ray analysis of ZnO nanoparticles by WilliamsoneHall and sizeestrain plot Methods -Solid State Sciences 13 (2011) 251e256.
[25] 22. R. Hepzi Pramila Devamani, M. Jansi Rani-Synthesis and Characterization of LeadChromate nanoparticles.-IJSR-Volume3 issue 4,April 2014,ISSN NO.2277-8179. 3 |
[26] 23. Y. T. Prabhu, K. Venkateswara Rao, V. Sesha Sai Kumar, B. Siva Kumari- X-ray Analysis of Fe doped ZnO Nanoparticles by Williamson-Hall and Size-Strain Plot Methods -International Journal of Engineering and Advanced Technology (IJEAT) ISSN: 2249 – 8958, Volume-2, Issue-4, April 2013.
[27] 24. A. Habiba,∗, R. Haubnerb, N. Stelzer- Effect of temperature, time and particle size of Ti precursor on hydrothermal synthesis of barium titanate -Materials Science and Engineering B 152 (2008) 60–65.
[28] 25.Vinila, V.S., Jacob, R., Mony, A., Nair, H.G., Issac, S., Rajan, S., Nair, A.S. and Isac, J. (2014) XRD Studies
[29] on Nano Crystalline Ceramic Superconductor PbSrCaCuO at Different Treating Temperatures. *Crystal Structure Theory andApplications*,3,1-9.http://dx.doi.org/10.4236/csta.2014.